

## Supplementary Information

# Chloride ions as integral parts of hydrogen bonded networks in aqueous salt solutions: the appearance of solvent separated anion pairs

Ildikó Pethes<sup>a</sup>, Imre Bakó<sup>b</sup>, László Pusztai<sup>a,c</sup>

<sup>a</sup>Wigner Research Centre for Physics, Konkoly Thege út 29-33., H-1121 Budapest, Hungary

<sup>b</sup>Research Centre for Natural Sciences, Magyar tudósok körútja 2, H-1117 Budapest, Hungary

<sup>c</sup>International Research Organisation for Advanced Science and Technology (IROAST),  
Kumamoto University, 2-39-1 Kurokami, Chuo-ku, Kumamoto 860-8555, Japan

Corresponding author: e-mail: [pethes.ildiko@wigner.hu](mailto:pethes.ildiko@wigner.hu)

## I. On the ionic/covalent character of Cl<sup>-</sup>...H-O hydrogen bonds: quantum chemical considerations

Hydrogen bonding (H-bonding) is an important interaction that plays a key role in chemical, physical, and biochemical processes. H-bonding is significantly weaker than a typical chemical bond, but stronger than van der Waals interactions.

From the point of view of the present work, it would be essential to know (and demonstrate) that the interaction between chloride anions and water molecules, indeed, show characteristics of hydrogen bonds. Although quite some heuristic arguments are mentioned in the main text, we wished to provide further evidence in support of the claim. In this small demonstration, we use the ‘Atom in Molecule’ (AIM) [1 - 4] and ‘Natural Bond Orbitals’ (NBO) [5 - 8] approaches for characterizing the chloride ion - water interaction.

Bader’s theory [1] of atoms-in-molecules (AIM) is an elegant theoretical tool for understanding both covalent and non-covalent molecular interactions. Within the framework of this theory, one can investigate topological properties of the electron density in the molecule. One of the most important feature in this theory the existence of the bond critical point along a bond. It has already been shown that there is a correlation between the strength of the hydrogen bonding interaction and the properties at this point (charge density,  $\rho$ ; ellipticity, ...). In a weak/medium hydrogen bond the charge density is in the range of 0.002..0.04 and the Laplacian of the electron density,  $\Delta\rho$ , is positive (0.02..0.13), when using the definition of Popelier et al. [3].

The Natural Bond Orbitals method provides us with a deeper insight of the electron transfer process from the lone pair of a Lewis base to an unfilled OH\* antibonding orbital of a Lewis acid. This type of interaction can stabilize ‘complexes’, like the hydration shells of chloride ions. Both the AIM and NBO based calculations of the real charge on the chloride anion may quantitatively yield a hint on the strength/covalent character of an H-bond.

The geometries of Cl<sup>-</sup>...(H<sub>2</sub>O)<sub>6</sub> surface clusters were optimized at the M052x/cc-pvtz level of theory, which method is suitable for such calculations [9]. The initial cluster geometries were taken from the literature [10 - 12]. Properties of three different inner shell clusters were also investigated. The clusters considered here are shown in Figure S1. The DFT geometry optimization and single point energy calculations were performed by utilizing the

Gaussian09E.01 [13] program package. For reference, some properties of water dimers have also been computed by the same method.

**Table S1.** AIM and NBO properties of the clusters (see Figure S1) considered.

|   | $\rho$ (AIM)      | $\Delta\rho$ (AIM) | ellipticity<br>(AIM) | Charge of the Cl <sup>-</sup> ion<br>AIM/NBO |
|---|-------------------|--------------------|----------------------|--|
| water dimer                               | 0.026             | 0.082              | 0.028                |  |
| Cl <sup>-</sup> ...6 water surface        | 0.023<br>(±0.006) | 0.052<br>(±0.006)  | 0.021 (±0.006)       | -0.82/-0.85                                  |
| Cl <sup>-</sup> ...6 water inner<br>shell | 0.016<br>(±0.002) | 0.045<br>(±0.003)  | 0.047 (±0.02)        | -0.80/-0.87                                  |

Table S1 contains the aforementioned AIM and NBO properties of the investigated clusters. It is clear from the both the AIM and NBO charges of Cl<sup>-</sup> that there is a significant charge transfer in these complexes shown in Figure S1. Also note that values for the other properties shown are in the range of the corresponding values calculated for water dimers.

That is, it may be concluded that the Cl<sup>-</sup>...H-O interaction is certainly not purely electrostatic but shows all characteristics of a ‘standard’ hydrogen bond.

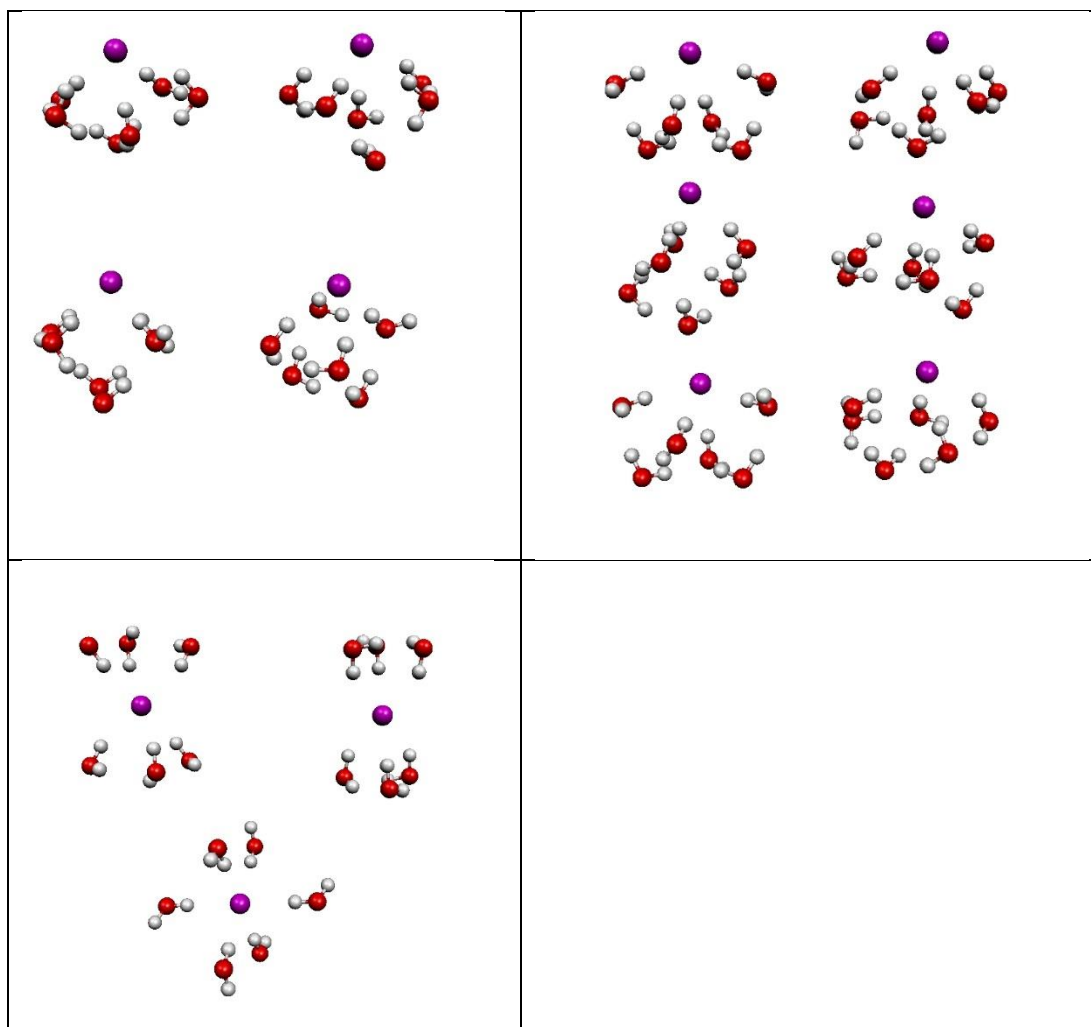


**Figure S1.** Clusters of  $\text{Cl}^-$  ions with 6 water molecules considered in this demonstration. Upper panels: anion on the surface; lower panel: anion in the inner shell.

## II. Molecular dynamics simulations

Classical molecular dynamics (MD) simulations were performed by the GROMACS software package (version 5.1.1) [14]. The calculations were performed at constant volume and temperature (NVT ensemble), at  $T = 300$  K. Cubic simulation boxes were used with periodic boundary conditions. Four different concentrations of aqueous LiCl solutions (from 3.74 mol/kg to 19.55 mol/kg) and pure water were investigated. The simulation boxes contained about 10000 atoms, the box lengths were calculated according to the experimental densities. The number of ions, water molecules, densities and box sizes are collected in Table 1 of the main text.

Pairwise additive non-polarizable intermolecular potentials was applied for the description of interatomic interactions. The non-bonded interactions are described by the Coulomb potential accounting for electrostatics and the 12-6 Lennard-Jones (LJ) potential for the van der Waals interactions:

$$V_{ij}(r_{ij}) = \frac{1}{4\pi\epsilon_0} \frac{q_i q_j}{r_{ij}} + 4\epsilon_{ij} \left[ \left( \frac{\sigma_{ij}}{r_{ij}} \right)^{12} - \left( \frac{\sigma_{ij}}{r_{ij}} \right)^6 \right]. \quad (1)$$

Here  $r_{ij}$  is the distance between particles  $i$  and  $j$ ,  $q_i$  and  $q_j$  are the point charges of the particles,  $\epsilon_0$  is the vacuum permittivity,  $\epsilon_{ij}$  and  $\sigma_{ij}$  are the 12-6 LJ potential parameters. Potential parameters applied in this study were chosen from the collection of Ref. [15], in which paper 29 force field models were compared according to their appropriateness to describe the structure of highly concentrated aqueous LiCl solutions.

The  $q_i$ ,  $\epsilon_{ii}$  and  $\sigma_{jj}$  parameters of six tested models are collected in Table S2, the parameters of the corresponding water models are shown Table S3. The  $\epsilon_{ij}$  and  $\sigma_{ij}$  values (parameters between unlike atoms) are calculated according to the Lorentz-Berthelot (LB) or the geometric (geom) combination rule, also shown in Table S2. In the geometric combination rule, both the  $\epsilon_{ij}$  and  $\sigma_{ij}$  are calculated as the geometric average of the homoatomic parameters, whilst in the Lorentz-Berthelot type the  $\epsilon_{ij}$  is calculated as geometric, and  $\sigma_{ij}$  as the arithmetic average of the relevant parameters.

**Table S2.** Force field parameters of the potential models investigated. The applied water models and combination rules are also shown. For the definitions of the combination rules, see the corresponding text.

| Model | $q_{\text{Li}}/q_{\text{Cl}}[e]$ | $\sigma_{\text{LiLi}}[\text{nm}]$ | $\varepsilon_{\text{LiLi}}[\text{kJ/mol}]$ | $\sigma_{\text{ClCl}}[\text{nm}]$ | $\varepsilon_{\text{ClCl}}[\text{kJ/mol}]$ | comb. rule | water model | References |
|-------|----------------------------------|-----------------------------------|--|-----------------------------------|--|------------|-------------|------------|
| JC-S  | +1/-1                            | 0.1409                            | 1.4089                                     | 0.4830                            | 0.0535                                     | LB         | SPC/E       | [16]       |
| JC-T  | +1/-1                            | 0.1440                            | 0.4351                                     | 0.4918                            | 0.0488                                     | LB         | TIP4PEw     | [16]       |
| MP-T  | +1/-1                            | 0.1715                            | 0.2412                                     | 0.4612                            | 0.1047                                     | LB         | TIP4PEw     | [17]       |
| AqCh  | +1/-1                            | 0.2126                            | 0.0765                                     | 0.4417                            | 0.4928                                     | geom       | SPC/E       | [18, 19]   |
| RM    | +1/-1                            | 0.3078                            | 0.0015                                     | 0.3771                            | 1.1137                                     | geom       | SPC/E       | [20]       |
| JJ    | +1/-1                            | 0.2870                            | 0.0021                                     | 0.4020                            | 2.9706                                     | geom       | TIP4P       | [21]       |

**Table S3.** Parameters of the water-models. In the TIP4P and TIP4PEw models there is a fourth (virtual) site (M). It is situated along the bisector of the H-O-H angle and coplanar with the oxygen and the hydrogen atoms. The negative charge is allocated to M.

|         | $\sigma_{\text{Oo}}[\text{nm}]$ | $\varepsilon_{\text{Oo}}[\text{kJ/mol}]$ | $q_{\text{H}}[e]$ | $d_{\text{O-H}}[\text{nm}]$ | $\theta_{\text{H-O-H}}[\text{deg}]$ | $d_{\text{O-M}}[\text{nm}]$ | Ref. |
|---------|---------------------------------|--|-------------------|-----------------------------|-------------------------------------|-----------------------------|------|
| SPC/E   | 0.3166                          | 0.6502                                   | +0.4238           | 0.1                         | 109.47                              | -                           | [22] |
| TIP4P   | 0.3154                          | 0.6485                                   | +0.52             | 0.09572                     | 104.52                              | 0.015                       | [23] |
| TIP4PEw | 0.3164                          | 0.6809                                   | +0.52422          | 0.09572                     | 104.52                              | 0.0125                      | [24] |

According to Ref. [15] the models' appropriateness to describe the structure of the highly concentrated aqueous LiCl solutions is more or less proportional to the number of the contact ion pairs predicted by the model. The tested six potential models were selected to cover the full range of the numbers of the contact ion pairs found in Ref. [15] (see Table S4).

**Table S4.** Average numbers of the contact ion pairs ( $N_{\text{LiCl}}$  coordination numbers) predicted by the force field models investigated in Ref. [15].

| forcefield | 3.74m | 8.3m | 11.37m | 19.55m |
|------------|-------|------|--------|--------|
| JC-S       | 0.01  | 0.08 | 0.24   | 1.28   |
| JC-T       | 0.08  | 0.31 | 0.59   | 1.47   |
| MP-T       | 0.46  | 0.93 | 1.27   | 1.86   |
| AqCh       | 1.28  | 1.67 | 1.83   | 2.15   |
| RM         | 1.95  | 2.26 | 2.32   | 2.51   |
| JJ         | 2.05  | 2.26 | 2.35   | 2.49   |

In the main text results obtained by using (one of) the best model(s), JC-S, a model of Joung and Cheatham, III [16], are presented. For comparison, data from a 'bad' model, RM, a

force field set of Reif and Hünenberger [20] is also discussed. Figure S2 demonstrates the difference between ‘good’ and ‘bad’ potential models. The ‘JC-S’ combination reproduces measured data, in the reciprocal space, at an at least semi-quantitative level: this combination is therefore used as ‘good’ combination in the main text.

During the simulations water molecules were kept together rigidly by the SETTLE algorithm [25]. Coulomb interactions were treated by the smoothed particle-mesh Ewald (SPME) method [26,27], using a 10 Å cutoff in direct space. The van der Waals interactions were also truncated at 10 Å, with added long-range corrections to energy and pressure [28].

Initial particle configurations were obtained by placing the ions and water molecules randomly into the simulation boxes. Energy minimization was carried out using the steepest descent method. After that the leap-frog algorithm was applied for integrating Newton’s equations of motion, using a 2 fs time step. The temperature was kept constant by the Berendsen thermostat [29] with  $\tau_T=0.1$  coupling. After a 4 ns equilibration period, particle configurations were collected in every 80 ps between 4 and 12 ns. The obtained 101 configurations were used for hydrogen bond analyses.

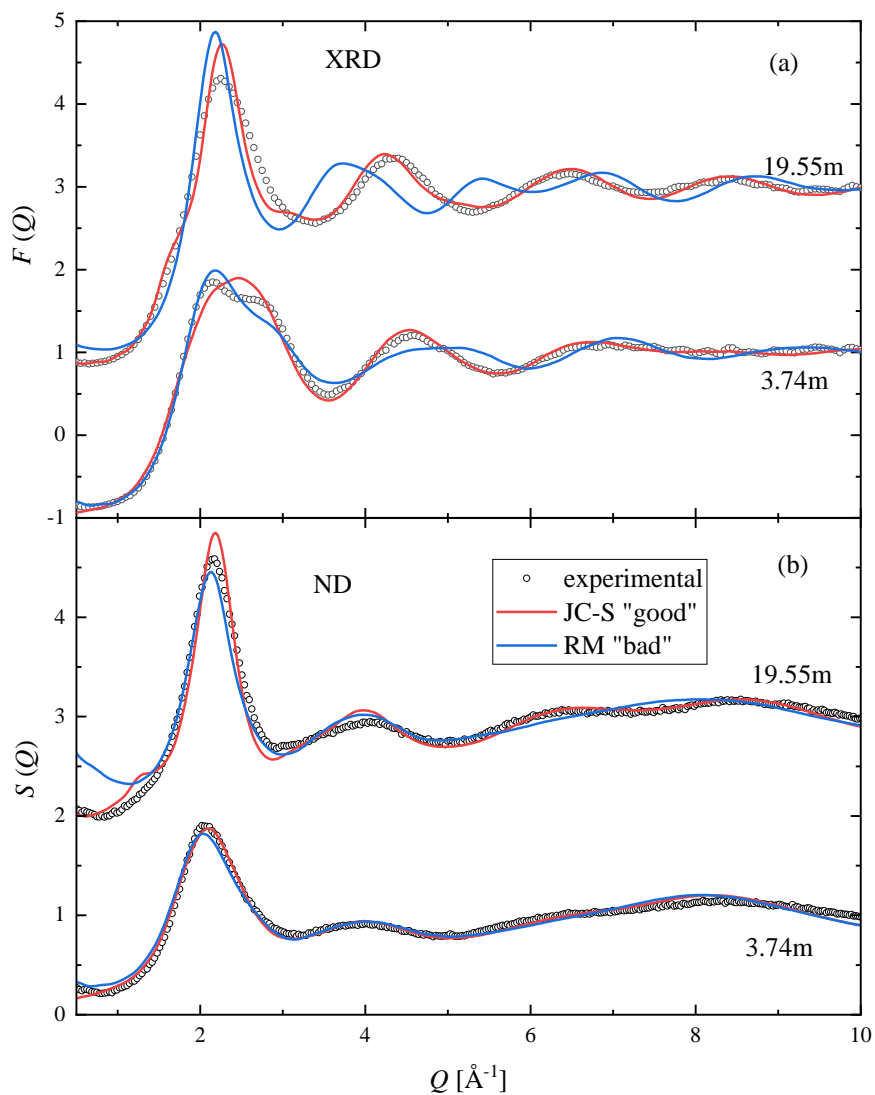


**Figure S2.** (a) X-ray and (b) neutron total structure factors from experiments (symbol, Ref. [30] ) and MD simulations using the JC-S (red) and the RM (blue) models for the 3.74m and 19.55m solutions.

### III. Cluster size distributions: ‘proof of concept’ – energetic definition of hydrogen bonds

In sections III., IV., VII., and VIII. we show the same kinds of graphs as Figures 1, 2, 3, 5 and 6 of the main text, but using the energetic definition of hydrogen bonds (see, e.g., Refs. [31 - 33]), instead of the purely geometric one that is utilized in the main text.

In short, the energetic definition of H-bonds works in conjunction with one simple geometric criterion as follows: two water molecules, as well as a chloride ion and a water molecule, are considered to be hydrogen-bonded to each other if they are found within a distance  $r(\text{O}\dots\text{H} / \text{Cl}\dots\text{H}) < 2.5 \text{ \AA}$ , and the interaction energy is smaller than  $-12 \text{ kJ/mol}$  (ca.  $-3 \text{ kcal/mol}$ ).

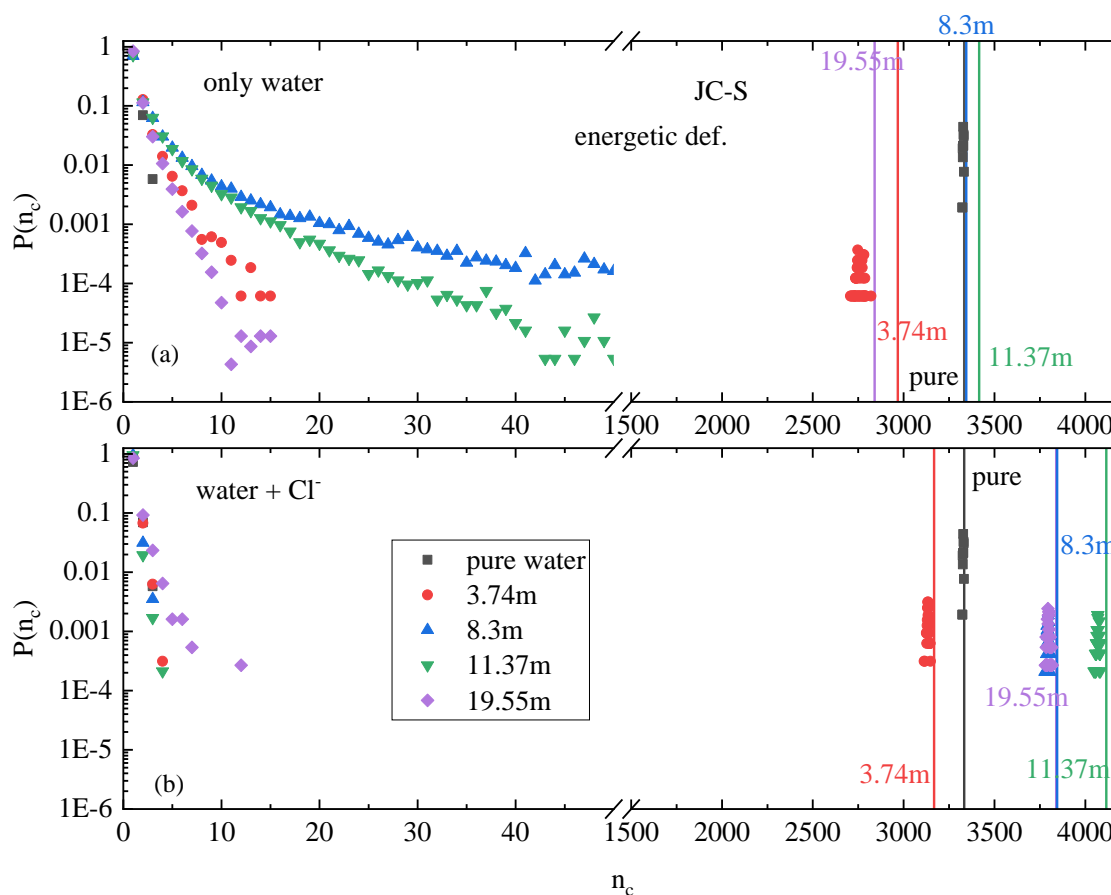


**Figure S3.** Cluster size distributions calculated for the same set of atomic configurations. (a) Water molecules only (no Cl<sup>-</sup> ions in the H-bonded network). (b) Water molecules AND chloride ions. (The vertical lines show the number of (a) water molecules (b) the Cl<sup>-</sup> ions plus water molecules in the system.) The JC-S potential model and the energetic definition of H-bond is used.

#### IV. Cyclic entities: ‘proof of concept’ – energetic definition of hydrogen bonds

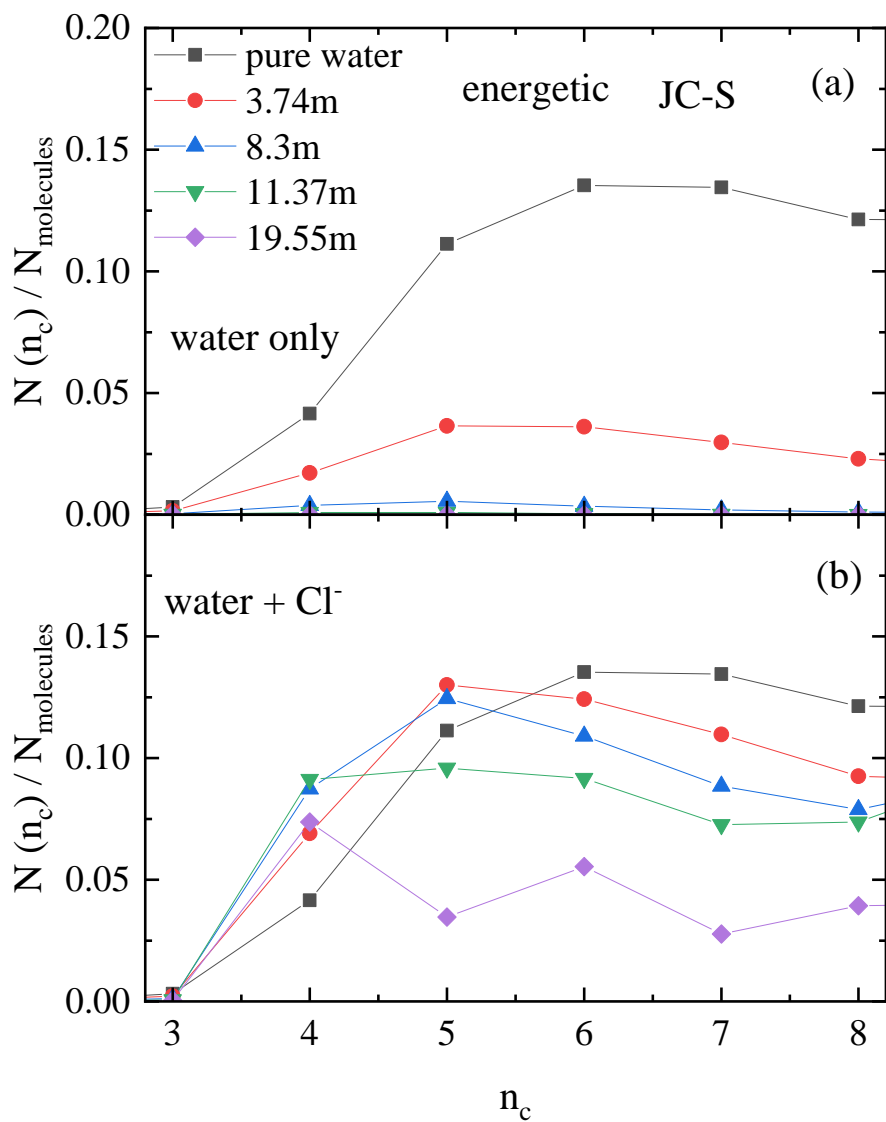


**Figure S4.** Size distribution of cyclic entities, as calculated for the same set particle configurations, but (a) without chloride ions, and (b) with chloride ions in the H-bonded network. The energetic definition of H-bond is used.

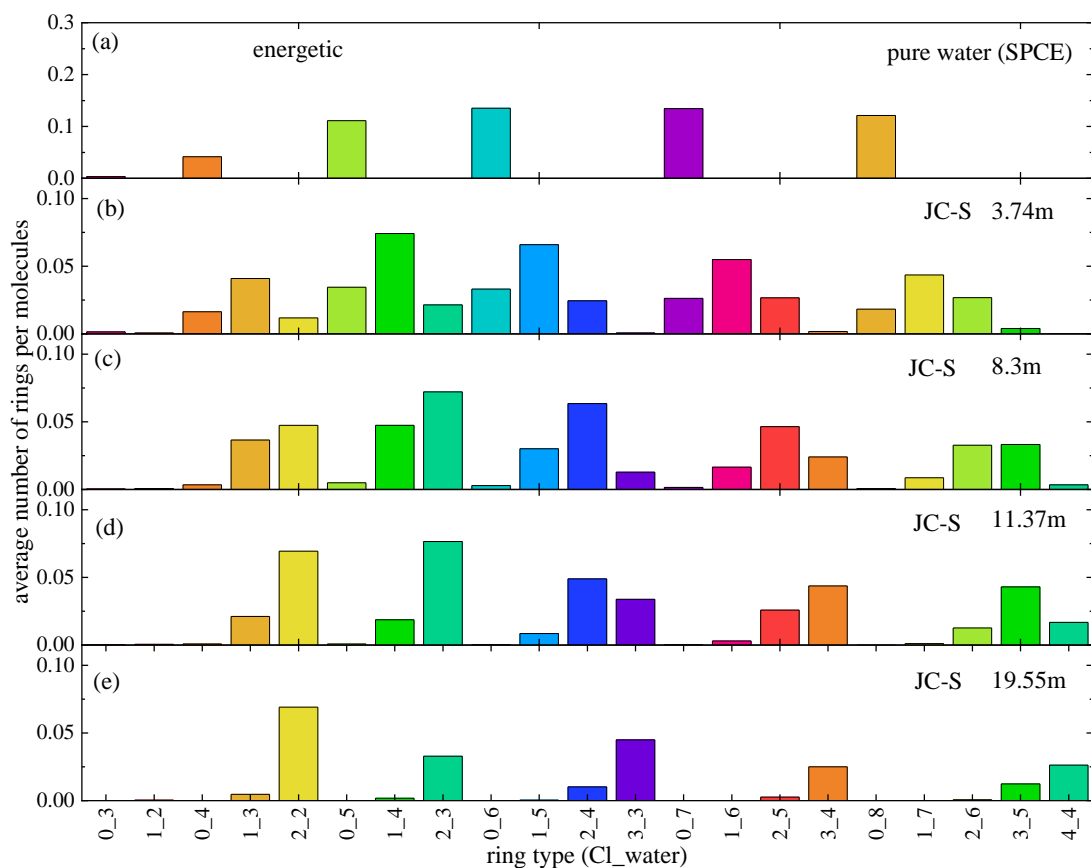


**Figure S5.** Distribution of different types of rings (rings contain Cl<sup>-</sup> ions and water molecules), normalized by the number of molecules (water + Cl<sup>-</sup> ions), at different concentrations obtained from JC-S model using the energetic definition of H-bond. Note: scaling in part (a) is different from that in the other parts.

## V. Hydrogen bond energetics

Bonding energies for single  $\text{Cl}^- \dots \text{O-H}$  bonds, as well as for those participating in solvent separated anion pairs have been calculated the same way as H-bond energies in, e.g. Refs. [32, 33].

Figure S6 contains the main findings of such calculations: at a given concentration, there is no difference between the energies of single  $\text{Cl}^- \dots \text{O-H}$  bonds and the ones that are parts of solvent separated anion pairs. On the other, energies of  $\text{Cl}^-$ -related H-bonds are getting somewhat deeper as LiCl concentration grows.

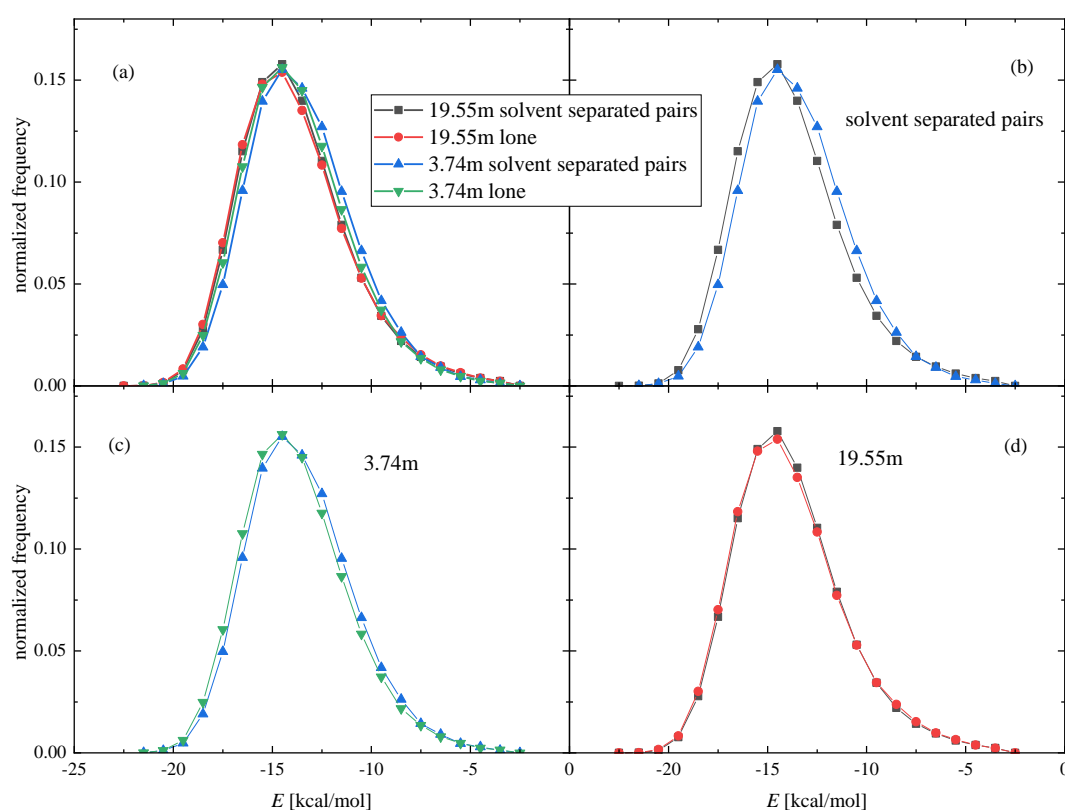


**Figure S6.** (a) Comparison of the hydrogen bond energies of  $\text{Cl}^-$  - water pairs in solvent separated anion pairs (in structural motifs in which the water molecules have two H-bonded  $\text{Cl}^-$  ion pairs) and in lonely  $\text{Cl}^-$  - water pairs (in motifs in which the water molecules have only one H-bonded  $\text{Cl}^-$  ion pair). (b) Comparison of the H-bond energies of  $\text{Cl}^-$  - water pairs in solvent separated anion pairs at different concentrations. (c) and (d) Comparison of the hydrogen bond energies of  $\text{Cl}^-$  - water pairs in solvent separated anion and in lonely  $\text{Cl}^-$  - water pairs in the (c) 3.74m and (d) 19.55m solutions.

## VI. On the lifetimes of solvent separated anion pairs

We have studied the surviving probability (lifetime of H-bonds, as well as of the ‘solvent-separated anion pairs’) similarly as in Ref. [33], calculated according to the following function [9, 34, 35]:

$$c_n = \frac{\langle \delta h_n^l(t) \delta h_n^l(0) \rangle}{\langle \delta h_n^l(0) \delta h_n^l(0) \rangle} \quad (2)$$

where

$$\delta h_n^l(t) = h_n^l(t) - \langle h_n^l(t) \rangle \quad (3)$$

The function  $h_n^l(t)$  has been defined in the following way:

$$h_n^l(t) = 1 \quad (4)$$

if a chloride ion or water molecule that was in the HB state  $n$  at time  $t = 0$  is in the same HB state at time  $t$ , irrespective of whether or not its HB state has changed in the meantime, and 0 otherwise.

An estimate for the lifetime of a given arrangement (single HB, or solvent-separated anion pair) from this correlation function can be obtained by the following formula[34, 35]:

$$\tau_n^l = \int c_n^l dt \quad (5)$$

Table S5 shows that the solvent separated anion pairs actually live (a little more 2 times) longer than single  $\text{Cl}^- \dots \text{H-O}$  hydrogen bonds. Another thing to note is that lifetimes grow drastically as the salt concentration approaches saturation (above 19.55 m).

**Table S5** Lifetimes (in picoseconds) of single  $\text{Cl}^- \dots \text{H-O}$  hydrogen bonds and of  $\text{Cl}^- \dots \text{H-O-H} \dots \text{Cl}^-$  solvent separated anion pairs in two of the aqueous LiCl solutions investigated here.

|  | lifetime (ps) | lifetime (ps) |
|--|---------------|---------------|
|  | 8.3 m         | 19.55 m       |
| $\text{Cl}^- \dots \text{H-O}$                     | 7.60          | 433.52        |
| $\text{Cl}^- \dots \text{H-O-H} \dots \text{Cl}^-$ | 19.39         | 907.84        |

Results for pure liquid water at 298 K, using the TIP4P/2005 model, may be taken as reference, see Table 4 and Fig. 11 of Ref. [33]. As the chloride ion related H-bonds are much longer lived, it is evident also from this comparison that the  $\text{Cl}^-\dots\text{H-O}$  hydrogen bond is stronger than the  $\text{O}\dots\text{H-O}$  one present in pure water.

## VII. Cluster size distributions: comparison of ‘good’ and ‘bad’ models – energetic definition of hydrogen bonds

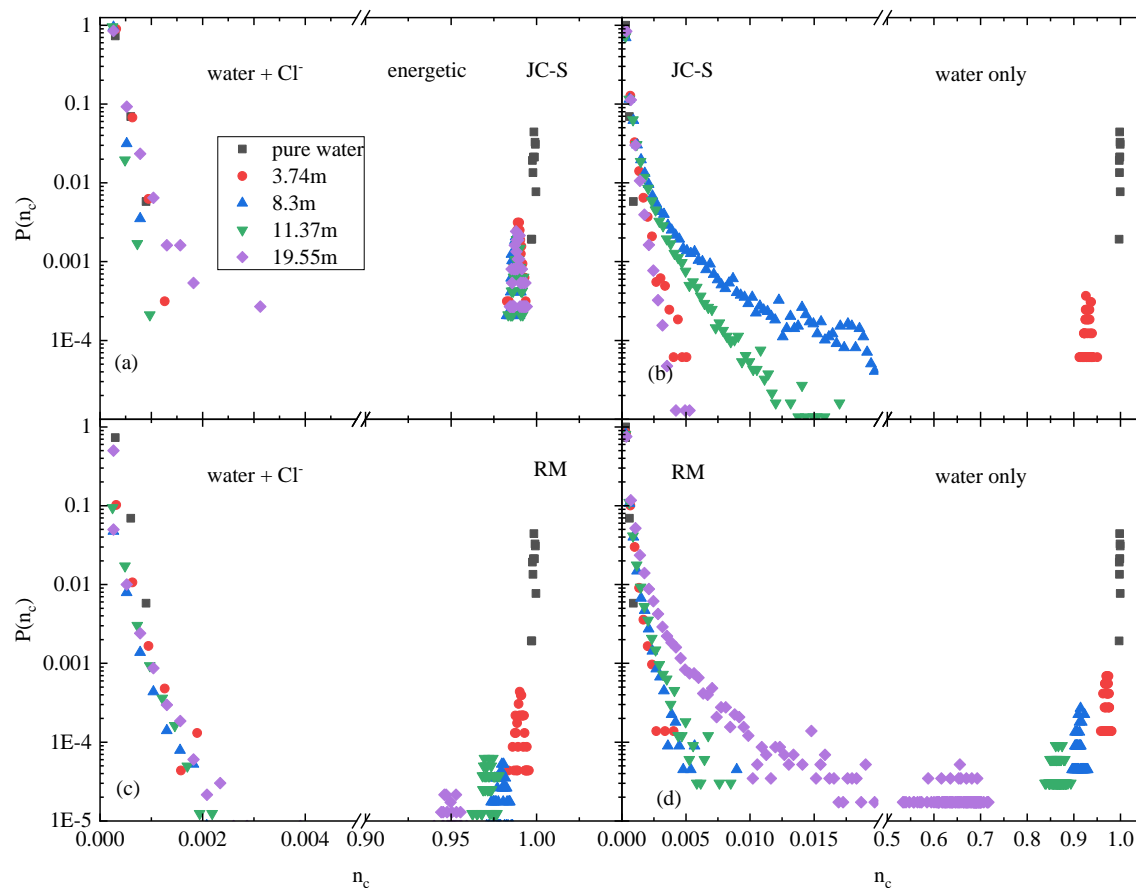


**Figure S7.** Cluster size distributions calculated for the atomic configurations obtained from (a, b) JC-S and (c, d) RM models. (a, c) Water molecules AND chloride ions. (b, d) Water molecules only (no  $\text{Cl}^-$  ions in the H-bonded network). (The x-axes are normalized by the cumulative numbers of (a, c)  $\text{Cl}^-$  ions plus water molecules, (b, d) water molecules in the configurations.) The energetic definition of H-bond is used.

## VIII. Cyclic entities: comparison of ‘good’ and ‘bad’ models – energetic definition of hydrogen bonds

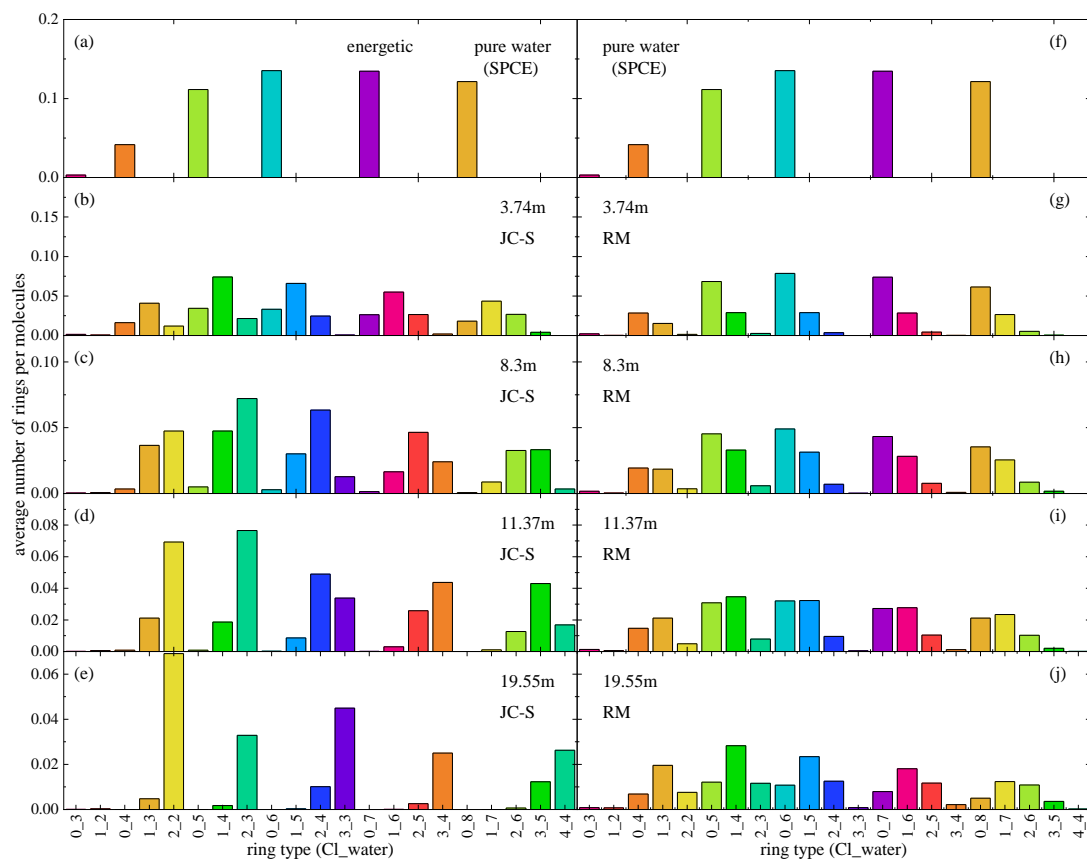


**Figure S8.** Distribution of different types of rings (rings contain  $\text{Cl}^-$  ions and water molecules), normalized by the number of molecules (water +  $\text{Cl}^-$  ions), at different concentrations, obtained from (b-e) JC-S and (g-j) RM models, using the energetic definition of H-bond. The ring size distribution in pure water (a,f) is also shown for reference.

## IX. Cluster size distributions: results for a range of potential models

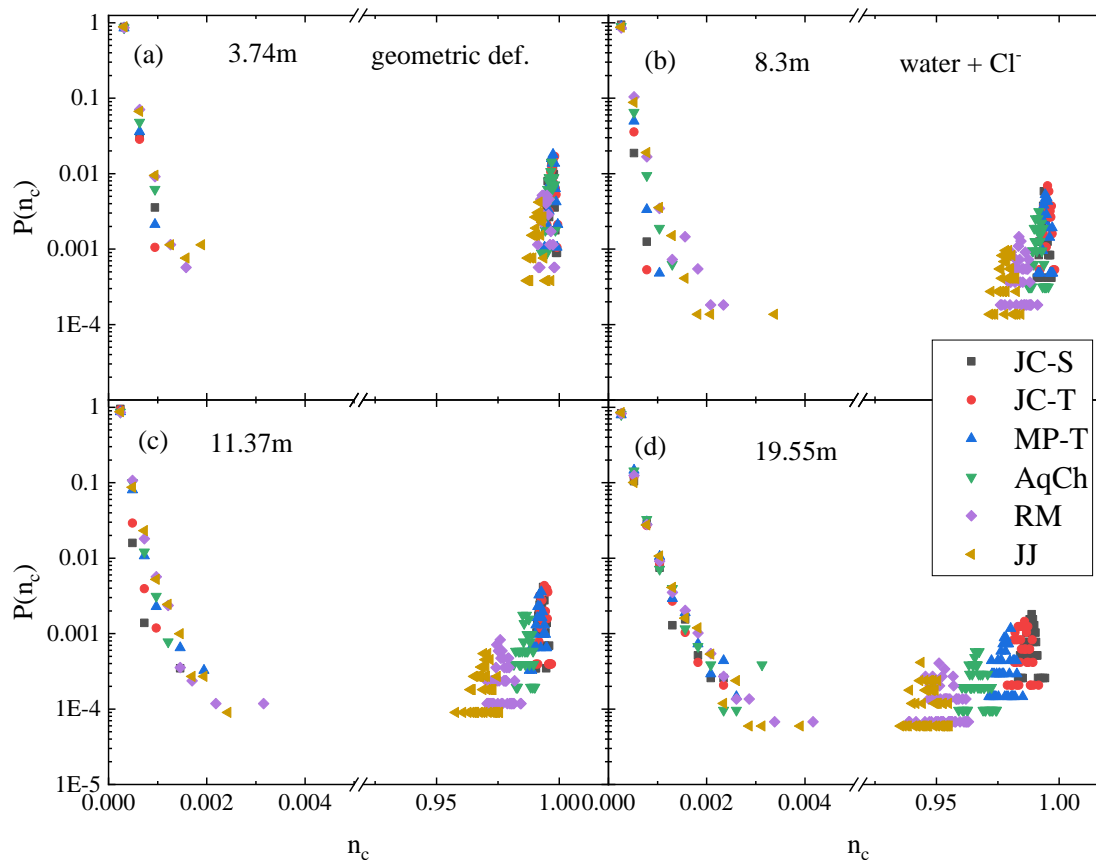


**Figure S9.** Cluster size distributions at various concentrations ( (a) 3.74 mol/kg, (b) 8.3 mol/kg, (c) 11.37 mol/kg, (d) 19.55 mol/kg) obtained from different MD models (using the geometric definition of H-bond). Water molecules AND chloride ions both are considered as parts of the network. (The x-axes are normalized by the cumulative numbers of Cl<sup>-</sup> ions plus water molecules in the configurations.)

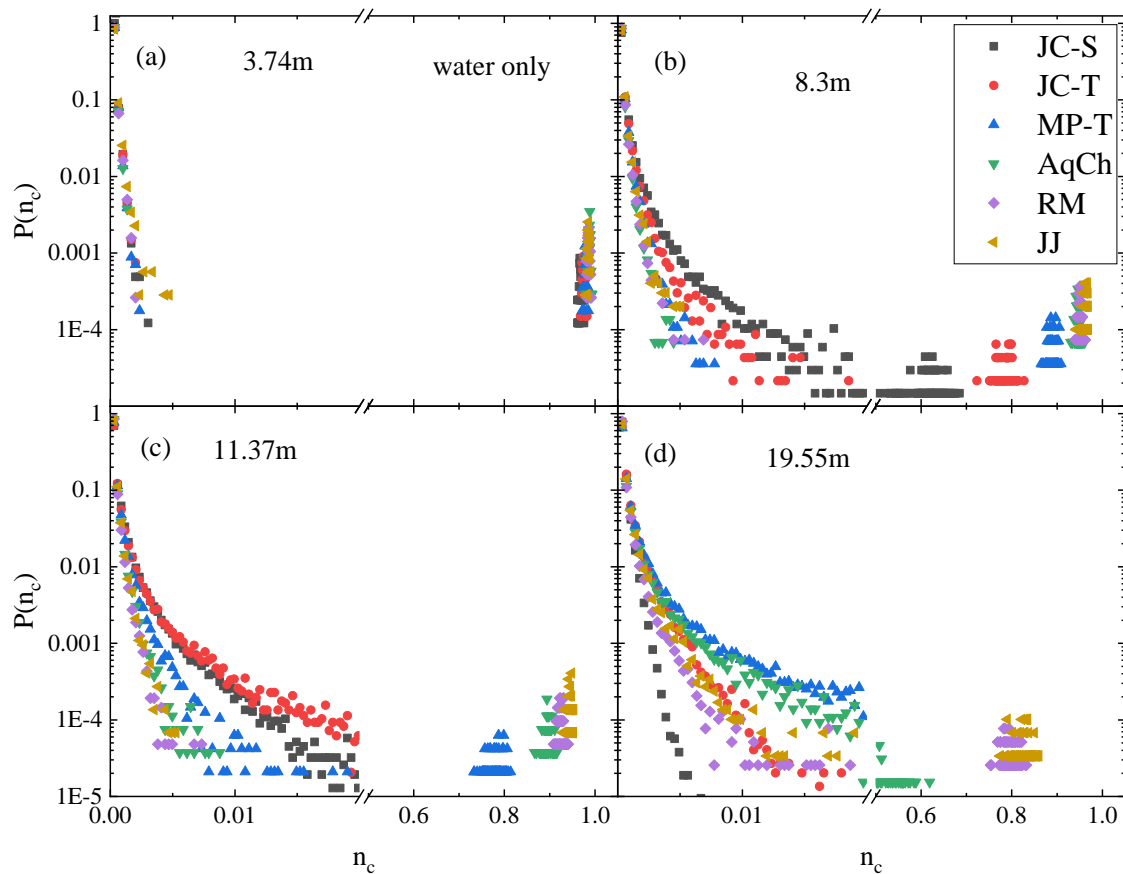


**Figure S10.** Cluster size distributions at various concentrations ( (a) 3.74 mol/kg, (b) 8.3 mol/kg, (c) 11.37 mol/kg, (d) 19.55 mol/kg) obtained from different MD models (using geometric definition of H-bonded molecules) Only water molecules are considered. (The x-axes are normalized by the numbers of water molecules in the configurations.)

## X. Cyclic entities: results for a range of potential models

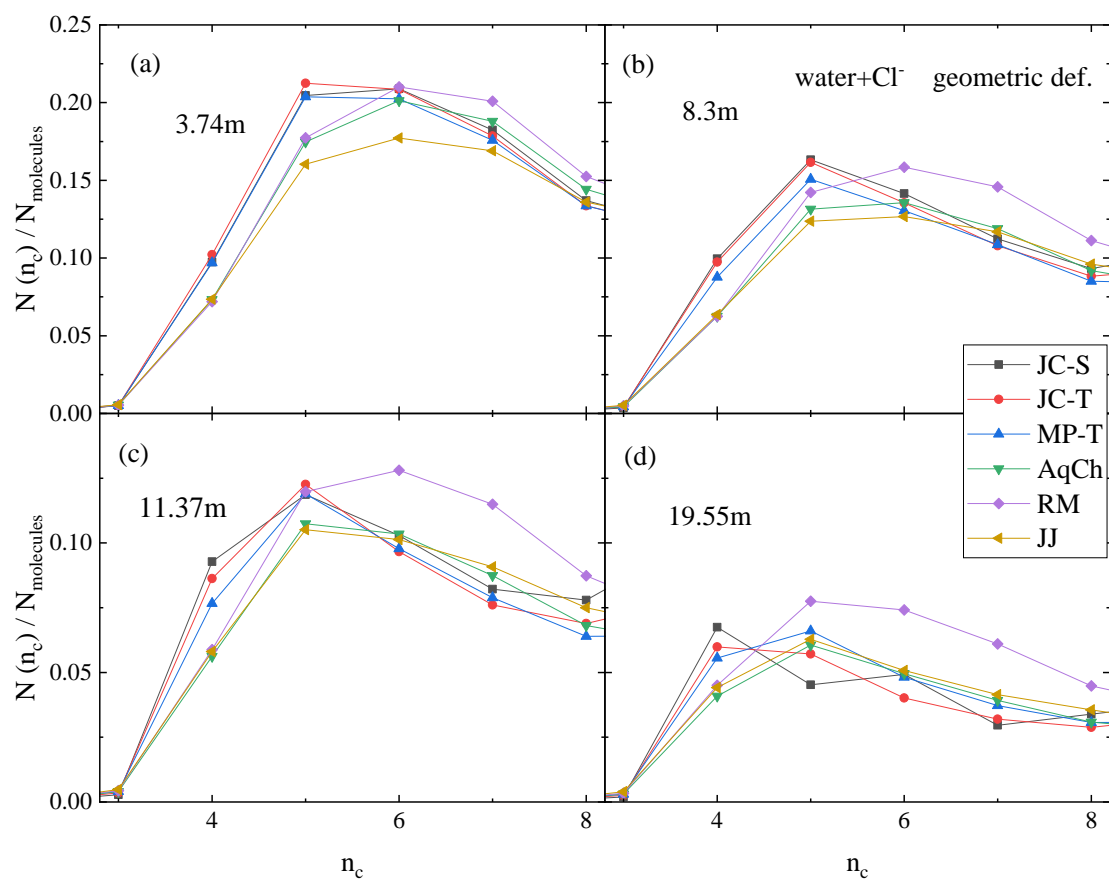


**Figure S11.** Size distributions of cyclic entities calculated with chloride ions in the H-bonded network at various concentrations ( (a) 3.74 mol/kg, (b) 8.3 mol/kg, (c) 11.37 mol/kg, (d) 19.55 mol/kg), obtained from different MD models (using the geometric definition of H-bond).

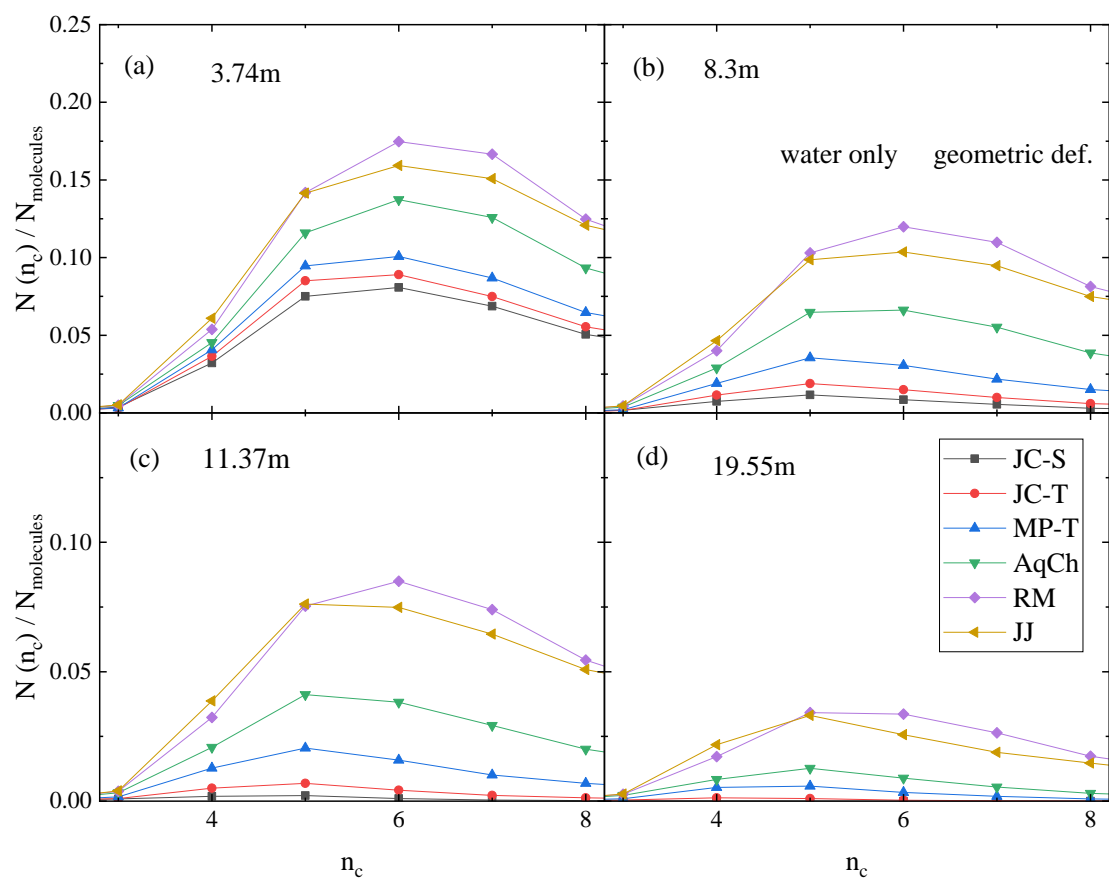


**Figure S12.** Size distribution of cyclic entities calculated without chloride ions in the H-bonded network, at various concentrations ( (a) 3.74 mol/kg, (b) 8.3 mol/kg, (c) 11.37 mol/kg, (d) 19.55 mol/kg), obtained from different MD models (using the geometric definition of H-bond).

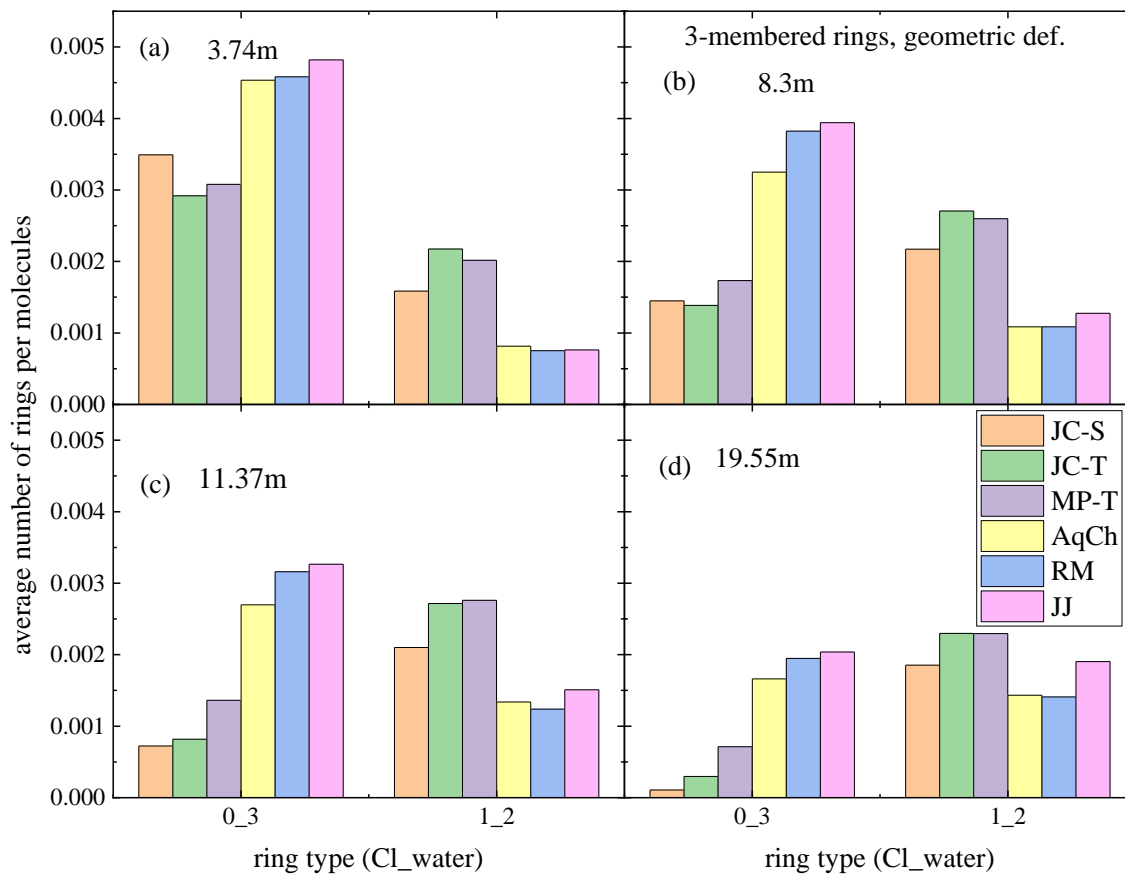


**Figure S13.** Distributions of different types of 3-membered rings (rings contain Cl<sup>-</sup> ions and water molecules), normalized by the number of molecules (water + Cl<sup>-</sup> ions), at different concentrations ( (a) 3.74 mol/kg, (b) 8.3 mol/kg, (c) 11.37 mol/kg, (d) 19.55 mol/kg), obtained from different MD models, using the geometric definition of H-bond.

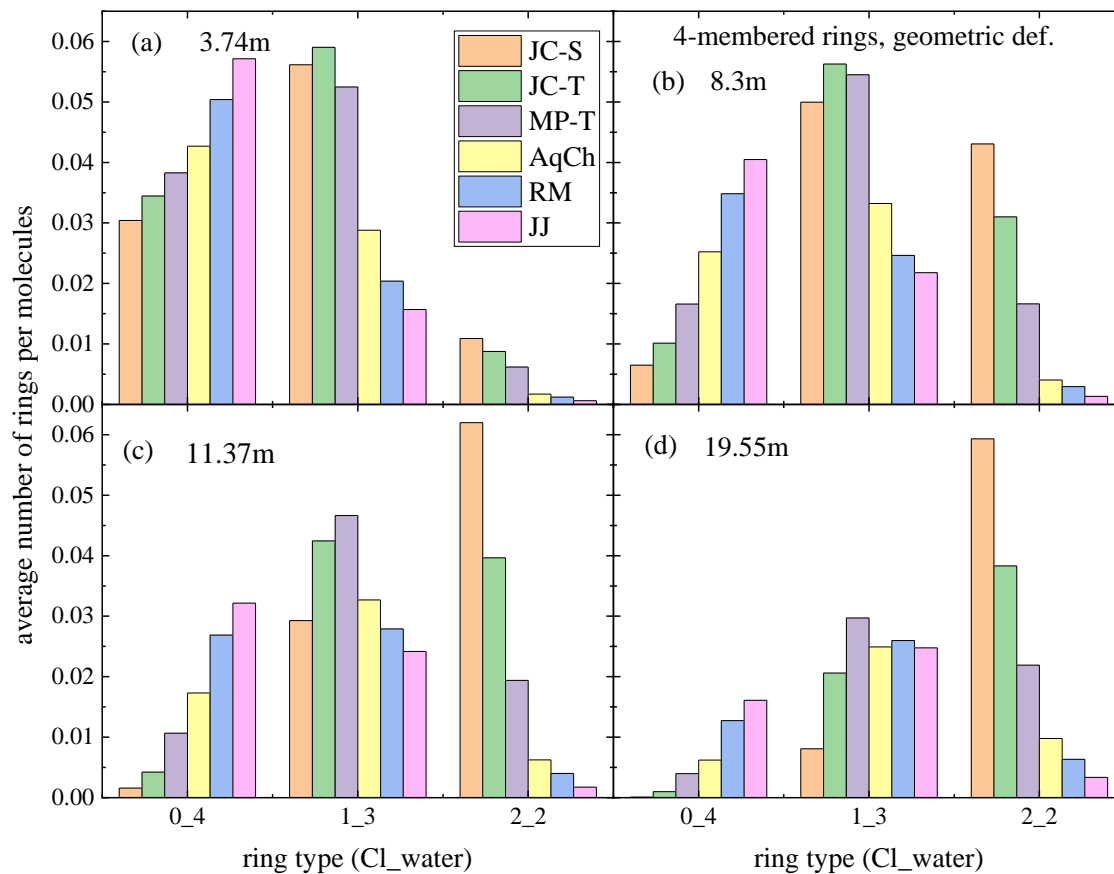


**Figure S14.** Distributions of different types of 4-membered rings (rings contain Cl<sup>-</sup> ions and water molecules), normalized by the number of molecules (water + Cl<sup>-</sup> ions), at different concentrations ( (a) 3.74 mol/kg, (b) 8.3 mol/kg, (c) 11.37 mol/kg, (d) 19.55 mol/kg), obtained from different MD models, using the geometric definition of H-bond.

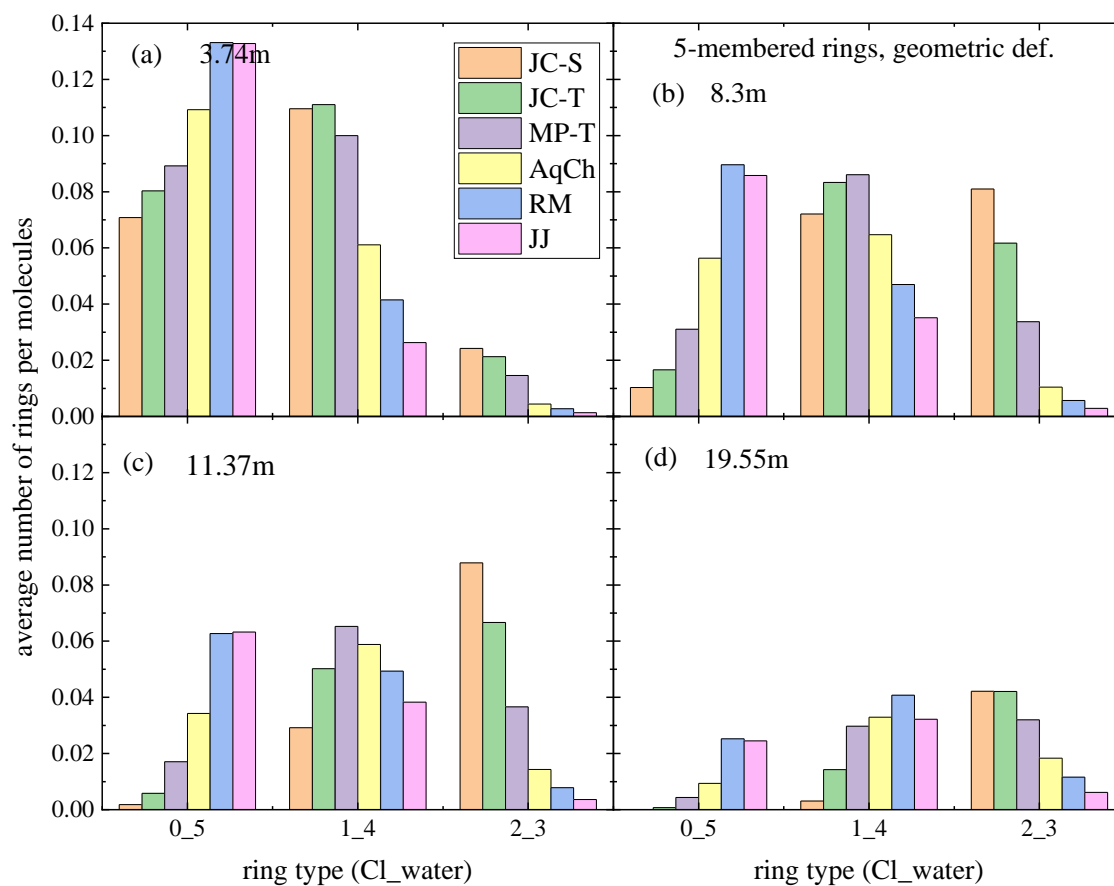


**Figure S15.** Distributions of different types of 5-membered rings (rings contain Cl<sup>-</sup> ions and water molecules), normalized by the number of molecules (water + Cl<sup>-</sup> ions), at different concentrations ( (a) 3.74 mol/kg, (b) 8.3 mol/kg, (c) 11.37 mol/kg, (d) 19.55 mol/kg), obtained from different MD models, using the geometric definition of H-bond.

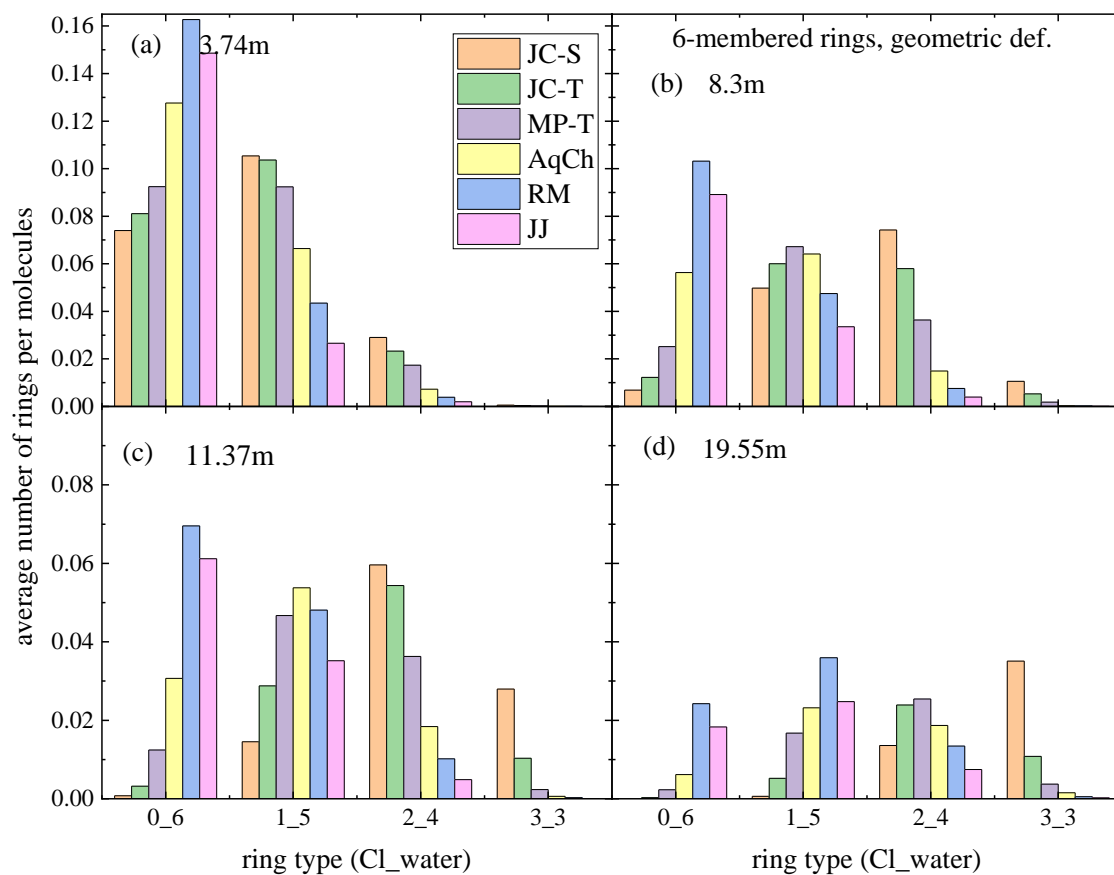


**Figure S16.** Distributions of different types of 6-membered rings (rings contain  $\text{Cl}^-$  ions and water molecules), normalized by the number of molecules (water +  $\text{Cl}^-$  ions), at different concentrations ( (a) 3.74 mol/kg, (b) 8.3 mol/kg, (c) 11.37 mol/kg, (d) 19.55 mol/kg), obtained from different MD models, using the geometric definition of H-bond.

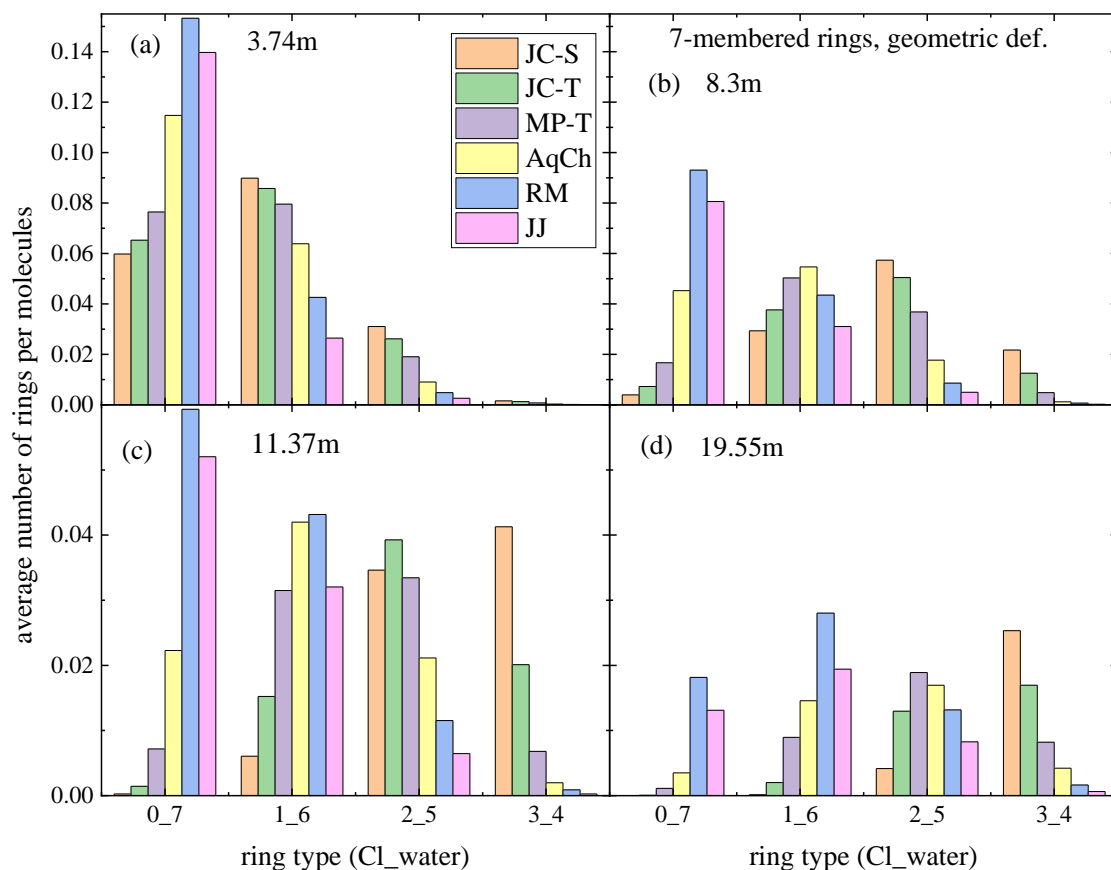


**Figure S17.** Distributions of different type 7-membered rings (rings contain Cl<sup>-</sup> ions and water molecules), normalized by the number of molecules (water + Cl<sup>-</sup> ions), at different concentrations ( (a) 3.74 mol/kg, (b) 8.3 mol/kg, (c) 11.37 mol/kg, (d) 19.55 mol/kg), obtained from various MD models, using the geometric definition of H-bond.

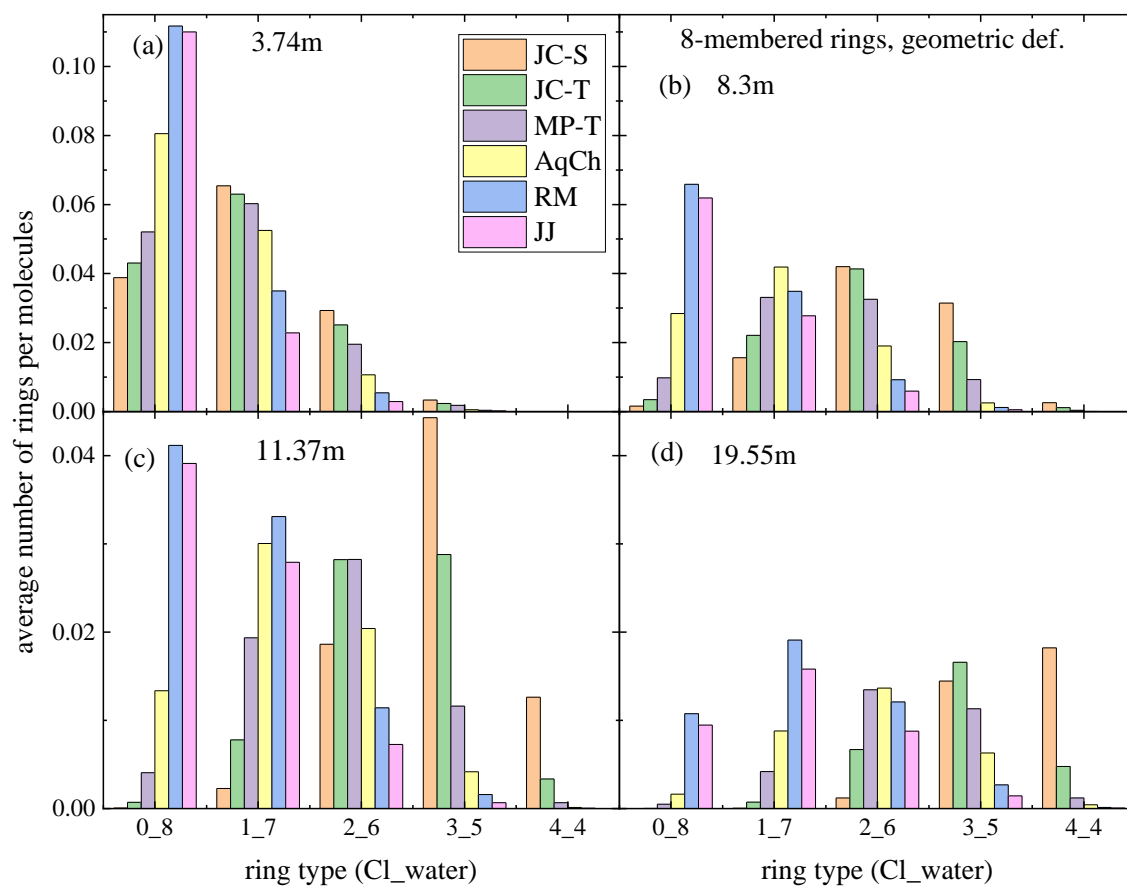


**Figure S18.** Distributions of different types of 8-membered rings (rings contain  $\text{Cl}^-$  ions and water molecules), normalized by the number of molecules (water +  $\text{Cl}^-$  ions), at different concentrations ( (a) 3.74 mol/kg, (b) 8.3 mol/kg, (c) 11.37 mol/kg, (d) 19.55 mol/kg), obtained from various MD models, using the geometric definition of H-bond.

## References

- 1 R. F. W. Bader, *Atoms in Molecules: A Quantum Theory*, Oxford University Press, Oxford, 1990.
- 2 U. Koch and P. L. A. Popelier, *J. Phys. Chem.*, 1995, **99**, 9747–9754.
- 3 P. L. Popelier, *Atoms in Molecules. An Introduction*, Pearson Education, Harlow, Great Britain, 2000.
- 4 M. Rozenberg, *RSC Adv.*, 2014, **4**, 26928–26931.
- 5 A. E. Reed, L. A. Curtiss and F. Weinhold, *Chem. Rev.*, 1988, **88**, 899–926.
- 6 F. Weinhold and C. R. Landis, *Valency and Bonding: A Natural Bond Orbital Donor-Acceptor Perspective*, Cambridge University Press, Cambridge, 2005.
- 7 Z. Zhang, D. Li, W. Jiang and Z. Wang, *Adv. Phys. X*, 2018, **3**, 1428915.
- 8 F. Weinhold, in *Advances in Protein Chemistry volume 72: Peptide Solvation and H-Bonds*, eds. R. L. Baldwin and D. Baker, Elsevier, Amsterdam, The Netherlands, 2005, pp. 121–155.
- 9 H.-S. Lee and M. E. Tuckerman, *J. Chem. Phys.*, 2007, **126**, 164501.
- 10 P. Bajaj, M. Riera, J. K. Lin, Y. E. Mendoza Montijo, J. Gazca and F. Paesani, *J. Phys. Chem. A*, 2019, **123**, 2843–2852.
- 11 G. Gilli and P. Gilli, *The Nature of the Hydrogen Bond*, Oxford University Press, Oxford, 2009.
- 12 S. J. Grabowski, Ed., *Hydrogen Bonding—New Insights*, Springer Netherlands, Dordrecht, The Netherlands, 2006.
- 13 Gaussian09E.01, <https://gaussian.com/products/>.
- 14 M. J. Abraham, T. Murtola, R. Schulz, S. Páll, J. C. Smith, B. Hess and E. Lindahl, *SoftwareX*, 2015, **1–2**, 19–25.
- 15 I. Pethes, *J. Mol. Liq.*, 2018, **264**, 179–197.
- 16 I. S. Joung and T. E. Cheatham, *J. Phys. Chem. B*, 2008, **112**, 9020–9041.
- 17 A. H. Mao and R. V Pappu, *J. Chem. Phys.*, 2012, **137**, 064104.

- 18 J. Chandrasekhar, D. C. Spellmeyer and W. L. Jorgensen, *J. Am. Chem. Soc.*, 1984, **106**, 903–910.
- 19 J. Åqvist, *J. Phys. Chem.*, 1990, **94**, 8021–8024.
- 20 M. M. Reif and P. H. Hünenberger, *J. Chem. Phys.*, 2011, **134**, 144104.
- 21 K. P. Jensen and W. L. Jorgensen, *J. Chem. Theory Comput.*, 2006, **2**, 1499–1509.
- 22 H. J. C. Berendsen, J. R. Grigera and T. P. Straatsma, *J. Phys. Chem.*, 1987, **91**, 6269–6271.
- 23 W. L. Jorgensen, J. Chandrasekhar, J. D. Madura, R. W. Impey and M. L. Klein, *J. Chem. Phys.*, 1983, **79**, 926–935.
- 24 H. W. Horn, W. C. Swope, J. W. Pitera, J. D. Madura, T. J. Dick, G. L. Hura and T. Head-Gordon, *J. Chem. Phys.*, 2004, **120**, 9665–9678.
- 25 S. Miyamoto and P. A. Kollman, *J. Comput. Chem.*, 1992, **13**, 952–962.
- 26 T. Darden, D. York and L. Pedersen, *J. Chem. Phys.*, 1993, **98**, 10089–10092.
- 27 U. Essmann, L. Perera, M. L. Berkowitz, T. Darden, H. Lee and L. G. Pedersen, *J. Chem. Phys.*, 1995, **103**, 8577–8593.
- 28 M. P. Allen and D. J. Tildesley, *Computer Simulation of Liquids*, Oxford University Press, Oxford, 1987.
- 29 H. J. C. Berendsen, J. P. M. Postma, W. F. van Gunsteren, A. DiNola and J. R. Haak, *J. Chem. Phys.*, 1984, **81**, 3684–3690.
- 30 I. Harsányi, L. Temleitner, B. Beuneu and L. Pusztai, *J. Mol. Liq.*, 2012, **165**, 94–100.
- 31 R. Kumar, J. R. Schmidt and J. L. Skinner, *J. Chem. Phys.*, 2007, **126**, 204107.
- 32 S. Pothoczki, L. Pusztai and I. Bakó, *J. Phys. Chem. B*, 2018, **122**, 6790–6800.
- 33 S. Pothoczki, L. Pusztai and I. Bakó, *J. Phys. Chem. B*, 2019, **123**, 7599–7610.
- 34 L. Saiz, J. A. Padro and E. Guardia, *Mol. Phys.*, 1999, **97**, 897–905.
- 35 A. Luzar and D. Chandler, *Phys. Rev. Lett.*, 1996, **76**, 928–931.